

Supporting Information

Dehydration of Molybdenum Oxide Hole Extraction Layers via Microwave Annealing for Efficiency and Lifetime Improvement in Organic Solar Cells

Anastasia Soultati^{a,b,*}, Ioannis Kostis^c, Panagiotis Argitis^a, Dimitra Dimotikali^b, Stella Kennou^d, Spyros Gardelis^e, Thanassis Speliotis^a, Athanassios G. Kontos,^a Dimitris Davazoglou^a, Maria Vasilopoulou^{a,**}

^aInstitute of Nanoscience and Nanotechnology (INN), National Centre for Scientific Research

“Demokritos”, 15310, Aghia Paraskevi Attikis, Athens, Greece

^bDepartment of Chemical Engineering, National Technical University of Athens, 15780 Athens, Greece

^cDepartment of Electronics, Technological Educational Institute (TEI) of Piraeus, 12244 Aegaleo, Greece

^dDepartment of Chemical Engineering, University of Patras, 26504 Patras, Greece

^eDepartment of Physics, University of Athens, 15784, Athens, Greece

*[*a.soultati@inn.demokritos.gr](mailto:a.soultati@inn.demokritos.gr), [**m.vasilopoulou@inn.demokritos.gr](mailto:m.vasilopoulou@inn.demokritos.gr)*

Table of Contents

Table S1 Indexing of the various peaks of XRD patterns of Mo oxides.....	S3
Figure S1 Tauc plot of the as-deposited and MW-annealed Mo oxide films	S4
Figure S2 Transmittance spectra of the as-deposited and MW-annealed Mo oxide films	S4
Figure S3 J-V curves of devices with MoO _x interlayers for different heating powers.....	S5
Figure S4 Absorption spectra of P3HT:PC ₇₁ BM films spin-coated on the different Mo oxide layers.....	S5
Figure S5 and Table S2 Contact angle measurements	S6
Figure S6 Variation of the refractive index of the as-deposited and MW-annealed Mo oxide films.....	S7
Figure S7 Variation of the extinction coefficient of the as-deposited and MW-annealed Mo oxide films ...	S7
Figure S8 Distribution of the normalized optical intensity of incident light within the device	S8

Table S1. Possible Mo oxides in MoO_x films and indexing of the various peaks observed in the XRD spectra in Figure 2 b of the main manuscript.

2θ (degrees)	Possible Compound	Crystallographic Plane
23.32	MoO ₃	[1 0 0], [0 2 0], [1 1 0]
	Mo ₉ O ₂₆	[-1 3 1], [-1 1 1]
25.07	Mo ₉ O ₂₆	[-2 1 1]
25.71	MoO ₃	[0 0 2], [0 2 0], [0 4 0], [2 1 0]
	Mo ₉ O ₂₆	[-1 1 2]
27.32	MoO ₃	[0 1 1], [0 2 1]
	Mo ₉ O ₂₆	[2 -3 1], [-3 1 0]
	Mo ₄ O ₁₁	[6 1 0]
	Mo ₉ O ₂₃	[1 1 2]
	Mo ₁₇ O ₄₇	[3 2 1]
38.99	MoO ₃	[1 0 2], [0 6 0], [0 2 0]
45.87	MoO ₃	[0 0 8], [2 0 0]
	Mo ₉ O ₂₃	[1 2 1]
49.24	MoO ₃	[0 2 0], [2 2 0], [0 0 2]
	Mo ₉ O ₂₆	[5 1 5]
51.48	Mo ₄ O ₁₁	[-8 1 3]
52.75	MoO ₃	[1 0 -4], [2 1 1], [0 8 0]
	Mo ₉ O ₂₆	[3 2 3]
	Mo ₄ O ₁₁	[2 3 1]
55.16	MoO ₃	[1 2 0], [0 2 2], [1 1 2]
	Mo ₉ O ₂₃	[3 1 6]
	Mo ₄ O ₁₁	[11 2 1]
61.71	MoO ₃	[2 6 0], [4 3 0]

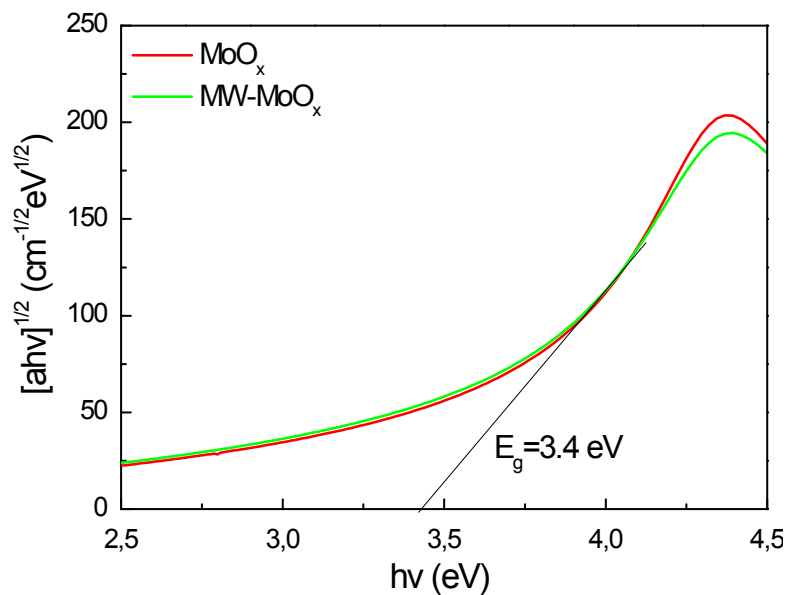


Figure S1 Tauc plot, as derived from absorption measurements, of 30 nm thick as-deposited hydrogenated under-stoichiometric and the microwave annealed Mo oxide films for the estimation of optical energy band gap.

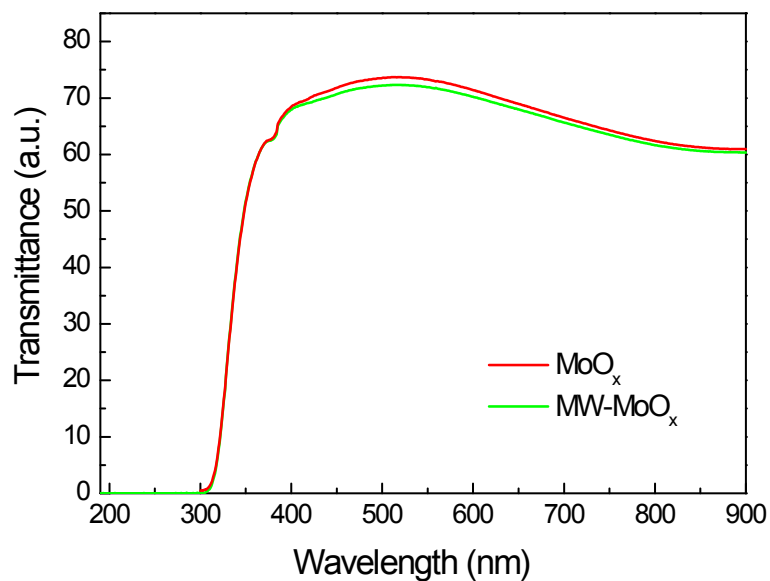


Figure S2 Transmittance spectra of the as-deposited Mo oxide film and the MW-annealed one deposited on glass/FTO substrates.

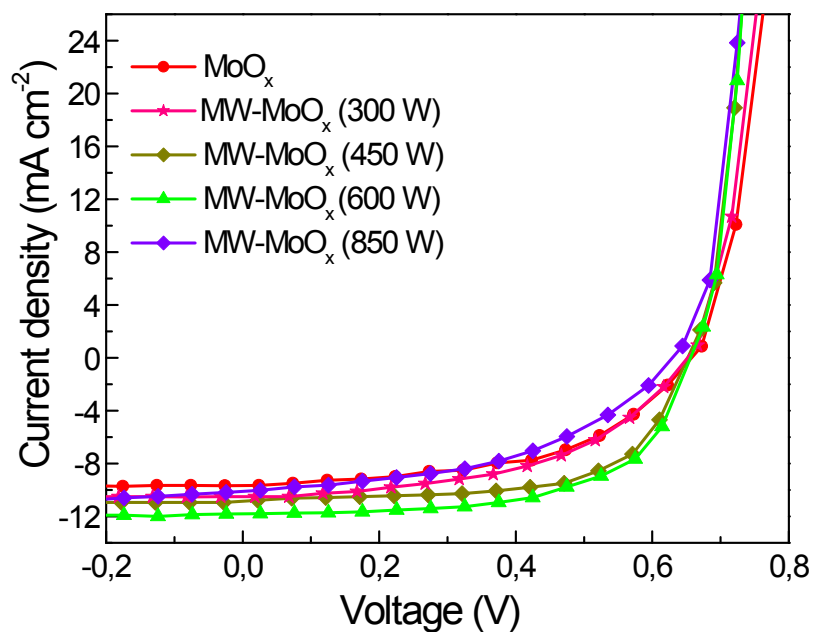


Figure S3 J-V curves of devices with MoO_x interlayers for different heating powers.

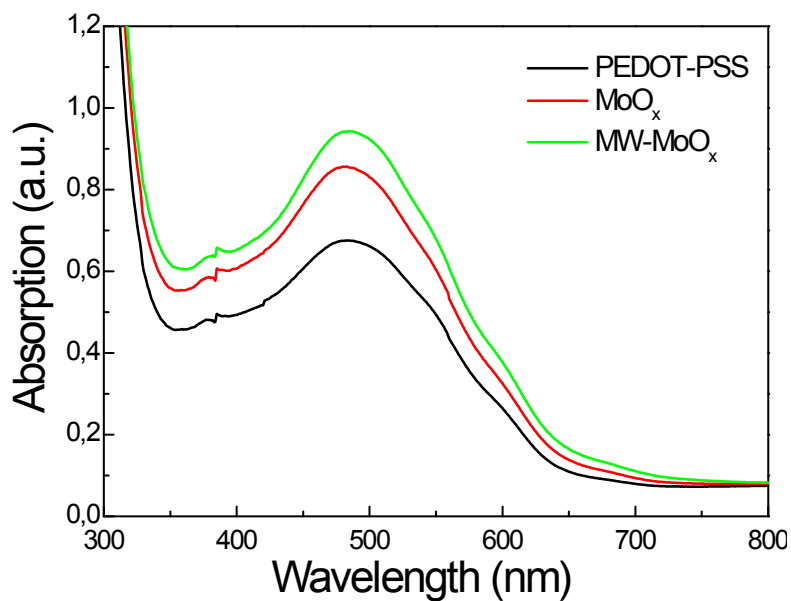


Figure S4 Absorption spectra of the P3HT:PC₇₁BM blend films spin-coated on Mo oxide layers subjected (or not) to microwave annealing after deposition.

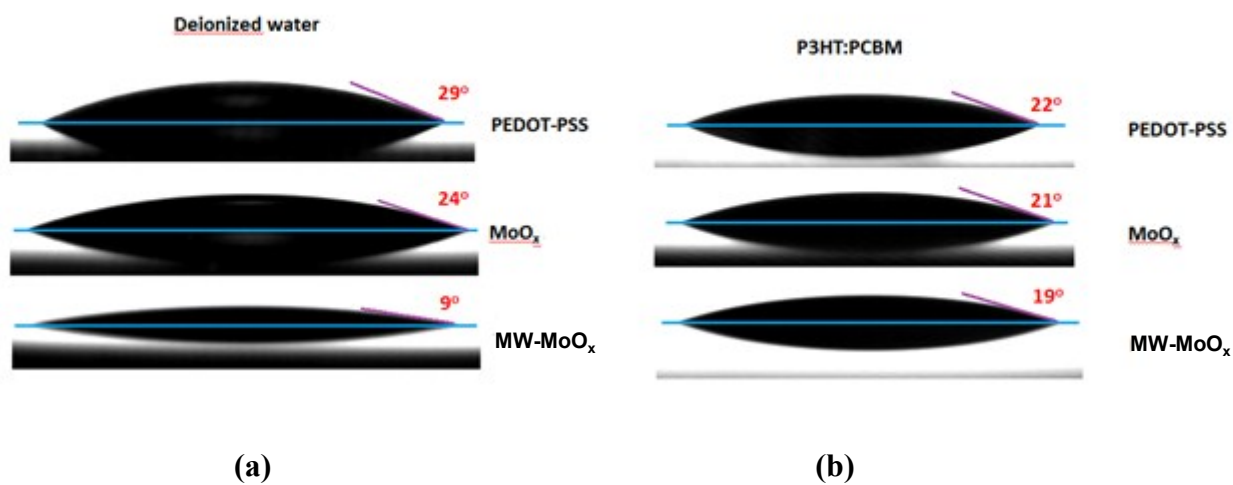


Figure S5 Measured contact angle between a drop of (a) deionized water and (b) P3HT:PC₇₁BM blend and Mo oxide films as deposited or being subjected to microwave annealing.

Table S2 Polar and non-polar components of surface energies of the PEDOT:SS, Mo oxide and MW-annealed Mo oxide substrates as calculated from contact angle measurements results.

Substrate	θ_w (°)	θ_i (°)	γ_s^p (mJ/m ²)	γ_s^d (mJ/m ²)	γ (mJ/m ²)
PEDOT:PSS	29.0	35.4	34.5	31.4	65.9
MoO_x	24.0	14.2	32.5	38.3	70.8
MW-MoO_x	9.0	12	37.5	37.9	75.4

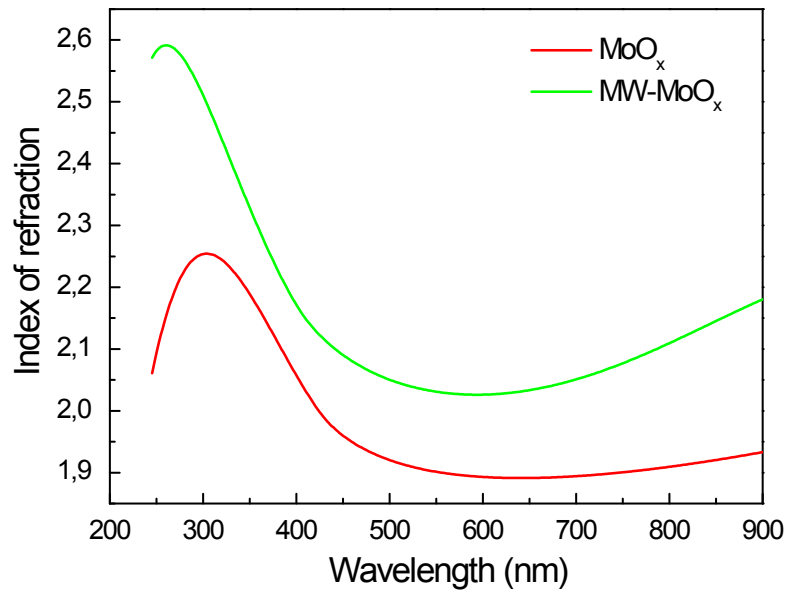


Figure S6 Variation of the refractive index of MoO_x and MW-annealed MoO_x films.

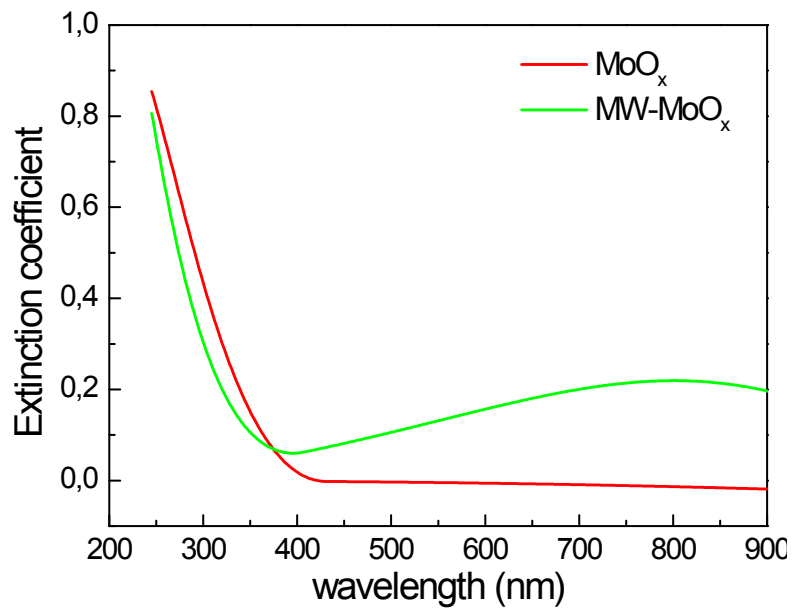


Figure S7 Variation of the extinction coefficient of MoO_x and MW-annealed MoO_x films.

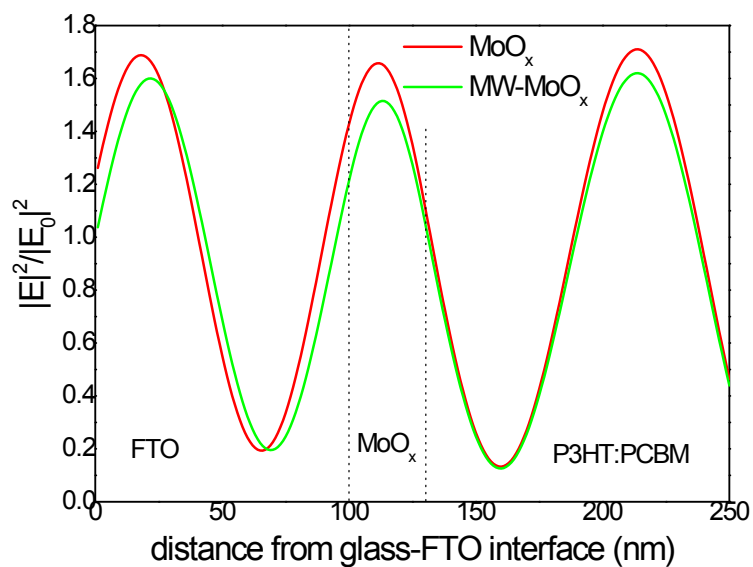


Figure S8 Distribution of the normalized optical intensity of incident light within the device (estimated for an incident light with a wavelength of 530 nm where the maximum of the photoactive blend absorption occurs).